

Biomechanical properties of intermediate filaments: from tissues to single filaments and back

Laurent Kreplak^{1*} and Douglas Fudge²

Summary

The animal cell cytoskeleton consists of three interconnected filament systems: actin-containing microfilaments (MFs), microtubules (MTs), and the lesser known intermediate filaments (IFs). All IF proteins share a common tripartite domain structure and the ability to assemble into 8–12 nm wide filaments. Electron microscopy data suggest that IFs are built according to a completely different plan from that of MFs and MTs. IFs are known to impart mechanical stability to cells and tissues but, until recently, the biomechanical properties of single IFs were unknown. However, with the discovery of naturally occurring micrometer-wide IF bundles and the development of new methodologies to mechanically probe single filaments, it is now possible to propose a more unified view of IF biomechanics. Unlike MFs and MTs, single IFs can now be described as flexible, extensible and tough, which has important implications for our understanding of cell and tissue mechanics. Furthermore, the molecular mechanisms at play when IFs are deformed point toward a pivotal role for them in mechanotransduction. *BioEssays* 29:26–35, 2007. © 2006 Wiley Periodicals, Inc.

Introduction

Cultured cells and tissues are sensitive to and shaped by mechanical stimuli.^(1–4) The sensing and transmission of a mechanical signal involves specialised transducer protein complexes as well as a network of interconnected cytoskeletal filaments that can also act as force transducers.⁽⁵⁾ While it is assumed that actin-containing microfilaments (MFs)⁽⁶⁾ and microtubules (MTs) play a major role in mechanotransduction, the third filamentous network forming the cytoskeleton, i.e. intermediate filaments (IFs), is generally neglected in this context, aside from a small number of papers.^(7–10) This is an interesting paradox since IFs have been considered for many years as “mechanical integrators of cellular space.”⁽¹¹⁾ This original statement was mainly based on the fact that, in a muscle cell, desmin IFs are attached to the nuclear surface, to the mitochondria, to the desmosomes and to the sarcomeres at the Z-disc.⁽¹²⁾ Such a spatial organization of IFs within cells makes them prime candidates for playing a role in mechanotransduction, providing they exhibit suitable biomechanical properties. Until recently, however, the field of IF mechanics was dominated by textile and cosmetic research on the tensile properties of hard α -keratin fibres like wool and hair, and very little was known about the mechanical properties of IFs in living cells.

The hard α -keratin fibre is a tough composite material consisting of aligned keratin IFs embedded in an isotropic, high-sulphur protein matrix⁽¹³⁾ that can occupy up to 40% of the fibre.^(14–16) In 1931 and 1933, Astbury and co-workers published the first X-ray diffraction study of hair structure at rest and under mechanical stress.^(17,18) Their main discovery was a molecular transformation that occurs when hair and wool fibres are stretched.⁽¹⁸⁾ Later, Pauling, Corey and Crick described the configuration of the keratin polypeptides within unstretched fibres as a double-stranded α -helical coiled-coil^(19,20) motif that is common to all IF proteins.⁽²¹⁾ Upon stretching a hard α -keratin fibre, the coiled coils, which have their axis parallel to the direction of applied stress, are transformed into a β -sheet structure with the β -strands running roughly parallel to the fibre axis.^(22,23) This is the so-called $\alpha \rightarrow \beta$ transition which is the cornerstone of all molecular models of hard α -keratin mechanics for extensions above 5%.^(24,25) In the elastic regime, wet wool and hair have a Young's modulus E

¹M.E. Müller Institute for Structural Biology, Biozentrum, University of Basel, Switzerland.

²Department of Integrative Biology, University of Guelph, Canada.

Funding agencies: L.K. was supported by a grant from the Swiss Society for Research on Muscular Diseases awarded to Ueli Aebi and Sergei Strelkov. D.F. was supported by a Natural Sciences and Engineering Research Council of Canada postdoctoral fellowship and a Seed Grant for Innovative Projects from the Faculty of Medicine at the University of British Columbia. This work was also supported by grants from the NCCR “Nanoscale Science”, the Swiss National Science Foundation, and the M.E. Müller Foundation, all awarded to Ueli Aebi.

*Correspondence to: Laurent Kreplak, M.E. Müller Institute for Structural Biology, Biozentrum, University of Basel, Klingelbergstrasse 70, CH-4056 Basel, Switzerland. E-mail: Laurent.kreplak@unibas.ch
DOI 10.1002/bies.20514

Published online in Wiley InterScience (www.interscience.wiley.com).

Abbreviations: Microfilaments, MFs; Microtubules, MTs; Intermediate filaments, IFs; Young's modulus, E; Gland Thread Cells, GTCs; Transmission electron microscopy, TEM; Atomic force microscopy, AFM.

of ~ 2 GPa,⁽²⁶⁾ and this was also assumed to be true for single keratin filaments and, by extension, for all IFs. Hence, IFs would be as rigid as F-actin ($E = 2.5$ GPa)^(27,28) and MTs ($E = 1$ GPa).^(27,29,30)

In reality, IFs directly isolated from cultured cells and tissues⁽³¹⁾ or assembled from purified proteins *in vitro*^(32,33) appear much more flexible than F-actin filaments and MTs when observed by electron microscopy.^(34,35) IFs are so much more flexible in fact that their highly curved appearance is used as a practical way of distinguishing them from other cytoskeletal filaments within whole tissue sections. In light of these observations, hair and wool may not be the best model to study IF biomechanics in the context of mammalian cell biology. In the following sections, we will review the main *in vitro* approaches that are currently yielding a better understanding of IF biomechanics and discuss recent *in vivo* evidence for the importance of IFs in determining the biomechanical properties of living cells.

In vitro assembled networks of IFs

Most of our knowledge of IF structure and assembly comes from the study of recombinant IF proteins that can be assembled into filaments *in vitro*. Comprehensive reviews on those topics can be found elsewhere.^(21,32,36) Here we will only briefly summarize the major relevant points. By electron microscopy (Fig. 1A,B), IFs appear typically as 8–12 nm wide smooth filaments built from the hierarchical association of 45–50 nm long dimers comprising a coiled-coil rod domain flanked by more flexible N- and C-terminal domains (Fig. 1C). Mature IFs are apolar and exhibit a shorter persistence length (~ 1 μm)⁽³⁴⁾ than F-actin filaments and MTs.^(37–39)

At protein concentrations above ~ 0.1 mg/ml, *in vitro* assembled IFs can be readily pelleted, embedded and

sectioned, thereby revealing a dense packing of filaments (100 to 1000 mg/ml) that have the tendency to align with their nearest neighbours^(40,41) (Fig. 1A). The morphology of the IFs in these pellets closely resembles that of cytokeratin IF networks within the stratum corneum, the outermost epidermal layer of skin in terrestrial vertebrates.⁽⁴²⁾ The biomechanical properties of dense IF pellets have never been studied. Instead, rheological measurements have been carried out with dilute (0.1 to 2 mg/ml) IF gels, in which a random network is formed by physical entanglement of the filaments (Fig. 1B). The pronounced ability of IFs to entangle stems from their greater flexibility than F-actin filaments and MTs, which in the absence of cross-linking proteins are less likely to form extended networks *in vitro*.

Gels formed from dilute suspensions of IFs differ dramatically in their mechanical properties from those formed by F-actin filaments and MTs.⁽⁴³⁾ Most strikingly, IF gels are much softer, more extensible and exhibit more dramatic strain hardening than gels formed by other kinds of biological filaments.⁽⁴⁴⁾ What can these results tell us about the biomechanical properties of single IFs? The high extensibility of IF gels likely arises from their low persistence length which, in turn, leads to more “slack” in the network, ultimately delaying the point where individual filaments are fully extended. Recent experimental⁽⁴⁵⁾ and simulation⁽⁴⁶⁾ results on the mechanics of semi-flexible polymer gels suggest that, at large strains, the majority of the stress developed by the gel can be attributed to the direct straining of relatively few filaments in tension. In light of these results, we propose that the high extensibility and dramatic strain hardening exhibited by IF gels suggest that IFs are capable of bearing considerably more longitudinal strain than other cytoskeletal filaments. For low strains, this alternative model is identical to the entropic gel model put forth by Coulombe et al.^(47–49) At high strains,

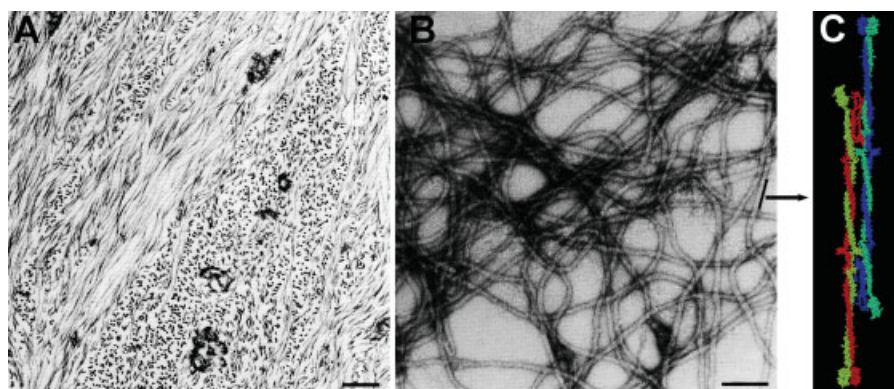


Figure 1. Electron micrographs of *in vitro* reconstituted vimentin IFs. **A:** Ultrathin section through a pellet, adapted from.⁽⁴¹⁾ **B:** Negatively stained preparation of vimentin IFs showing entanglements of filaments. The black bar highlights the approximate length of the building block, a vimentin tetramer, adapted from.⁽⁴¹⁾ **C:** An atomic model of a vimentin tetramer where the two coiled-coil dimers are clearly visible (courtesy of Sergei Strelkov). Bars, 200 nm in **(A)** and 100 nm in **(B)**.

however, we suggest that enthalpic forces arising from the direct longitudinal straining of IFs dominate the mechanics. One requirement of this new model is that individual IFs, unlike F-actin and MTs, must be able to withstand considerable longitudinal strain. While the stress–strain curve for a single IF is not yet known, a convenient experimental model, hagfish slime threads, is currently being used to take us one step closer to that goal.^(50,51)

Tensile properties of an IF bundle

Hagfishes are primitive bottom-dwelling proto-vertebrates that are renowned for their ability to give off liters of defensive slime when they are provoked.⁽⁵²⁾ The slime differs from other animal slimes in that it is permeated by thousands of very fine, very long protein threads, or slime threads.⁽⁵³⁾ These threads are manufactured in large, epidermally derived cells within the slime glands called Gland Thread Cells (GTCs)^(50,53,54) (Fig. 2). GTCs express massive amounts of keratin-like IF proteins, assemble them into IFs, and then anneal the IFs into a single, continuous slime thread that takes over the vast majority of the cell volume in mature cells.⁽⁵⁵⁾ During release of the slime exudate into seawater, entire GTCs are ejected via the holocrine mode along with membrane-bound mucin vesicles.^(52,56) In seawater, the GTCs lose their plasma membrane and unravel to a total length of about 15 cm.⁽⁵⁷⁾ It is the interaction of the GTCs with seawater and hydrated mucin vesicles that gives the slime its unique mechanical properties.⁽⁵⁷⁾ Individual slime threads are between 1 and 3 μm in diameter and consist almost exclusively of bundled IFs, with very little contamination by other proteins.^(53,54,57,58) Hence, slime threads are like very fine wool fibres, but without the high sulfur matrix. Individual GTCs can be isolated and unraveled

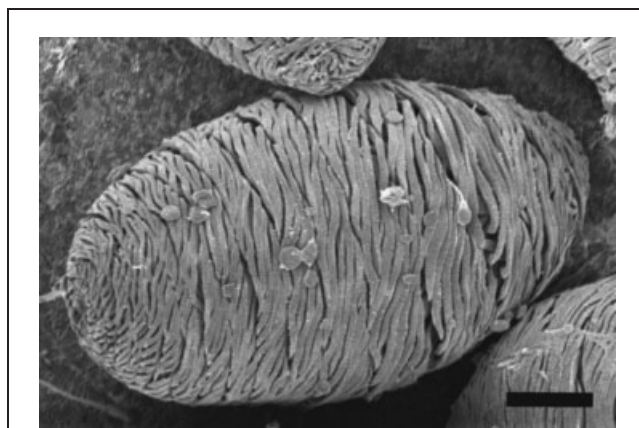


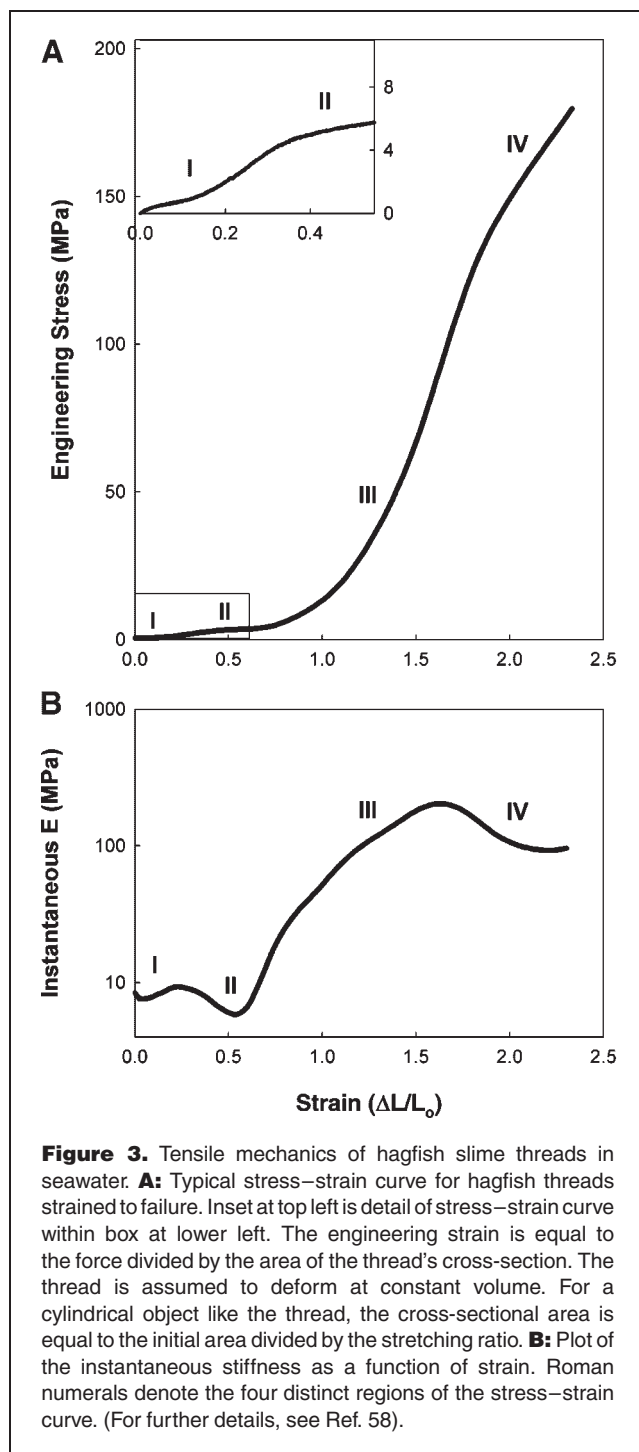
Figure 2. Scanning electron micrograph of a hagfish gland thread cell without its plasma membrane, exposing the intricately coiled slime thread. The slime thread consists of a solid, nearly pure bundle of 10^3 – 10^4 IFs in cross-section that can be unravelled and mounted in vitro for mechanical testing. Scale bar = 25 μm .

in vitro so that segments of slime thread can be used for mechanical testing.

One of the findings that came out of measuring slime thread mechanics was that the initial stiffness of a hydrated IF bundle is about 300 times lower than that of a hydrated wool fibre (6.4 MPa versus 2.0 GPa for hydrated wool).^(58,59) These results strongly contradict the assumption that IF biomechanics can be inferred from the mechanical properties of hydrated wool fibres, and suggest that hydrated IFs in cells may be far less stiff than previously assumed. Several findings in the IF biophysics literature that appeared anomalous in the old framework further support the “low stiffness” hypothesis. The first is that studies of IF structure in vitro have demonstrated that IFs possess low flexural stiffness, which can be estimated by analyzing the degree of curvature of IFs from TEM,⁽³⁸⁾ AFM⁽³⁴⁾ or light scattering⁽³⁷⁾ data. All these studies demonstrate that, in vitro, IFs exhibit a persistence length on the order of 1 μm , which is consistent with the flexibility of filaments as soft as slime threads, but far lower than what one would expect for 10 nm diameter filaments with the stiffness of wool. The second finding has to do with the behavior of the IF-rich stratum corneum. Its stiffness in water is about 700 times lower than that of hard α -keratin fibres like wool⁽⁶⁰⁾ and is remarkably similar to the stiffness of hagfish slime threads. This low initial stiffness of the stratum corneum is also broadly consistent with the dynamic shear modulus of diluted IF gels for small deformations.^(43,47,49)

The low initial stiffness of slime threads is just one aspect of a complex tensile behavior that is characterized by a non-linear stress–strain curve (Fig. 3).⁽⁵⁸⁾ By plotting the instantaneous stiffness as a function of strain (Fig. 3B), four mechanical regimes become apparent. The first is the low stiffness regime described above (region I), which is followed by an even lower stiffness ‘yield’ region (region II). In region III, stiffness rises dramatically. X-ray diffraction data suggest that regions II and III correspond to the disruption of coiled-coil α -helices in IF proteins, and the formation of stable β -sheet crystallites.⁽⁵⁸⁾ In region IV, stiffness levels off until failure.

In addition to their low initial stiffness, several aspects of slime thread tensile mechanics differ significantly from hydrated wool fibres. The average breaking strain, or ‘extensibility’ of slime threads is 220%, which means that they elongate to more than three times their initial length before they break. In contrast, the extensibility of hydrated wool fibres is only 45% at room temperature.⁽⁶¹⁾ Failure of slime threads occurs at a stress of about 180 MPa, which makes them comparable to wool fibres, and stronger than F-actin filaments (25 MPa based on the single filament data obtained by Tsuda et al).⁽⁶²⁾ With wool fibres, the drop in initial stiffness or ‘yield’ occurs at about 2.5% extension,⁽²⁵⁾ whereas in slime threads it occurs at 34% extension.⁽⁵⁸⁾ Both slime threads and wool fibres exhibit nearly perfect recovery from pre-yield



deformations, although this behavior is likely governed by different molecular mechanisms in the two materials.⁽⁶¹⁾ Another important difference is that wool fibres exhibit almost perfect recovery from post-yield deformations, whereas post-yield deformation in slime threads is for the most part plastic and hence leads to an irreversible deformation of the fibre. The

lack of post-yield recovery in slime threads is likely mediated by the formation of stable β -sheet crystallites which, in turn, lock the IFs in a new resting length. While it has been assumed for decades that post-yield deformation of wool also corresponds to an $\alpha \rightarrow \beta$ transition, recent evidence suggests that β -sheets do not readily form at room temperature in hydrated wool and hair.⁽⁶³⁾ Instead, the loss of α -helical structure coincides with an increase in random coil structure.⁽²³⁾ Hence, it is conceivable that the compressive forces exerted on extended coiled coils by the keratin matrix along with limited water availability, return IFs in wool to their resting length before stable β -sheets have a chance to form.⁽⁶¹⁾

While these results suggest that slime threads may be a better model for estimating IF mechanics than hydrated wool, they also raise the question of why slime threads differ so much in their biomechanical properties from wool fibres, which consist predominantly of IFs. One possibility is that the IFs in wool and other hard α -keratins are kept in a semi-dehydrated state that keeps both their stiffness and yield stress high. This hypothesis is supported by the fact that the mechanical properties of hydrated wool fibres are quite similar to those of slime threads tested in air.⁽⁶¹⁾

Slime threads will be used in future studies as a model system to quantify the influence of hydration water and filament-associated water on the mechanical properties of IFs. Slime threads may also be the optimal model for studying the effect of mechanical stress on IF protein conformation.⁽⁵⁸⁾ Hence the hagfish model is useful for exploring the biomechanical properties of IF bundles, but it is also important for generating novel and specific hypotheses about the behavior of single IFs. Obviously the next step will be to probe the mechanical behavior of single IFs *in vitro*, which is something that researchers have only recently accomplished for the first time.

Single IF biomechanics

With the development of micromanipulation tools such as optical tweezers and microlevers, it has become possible to estimate the mechanical properties of individual actin filaments⁽⁶⁴⁾ and microtubules.⁽²⁹⁾ For both types of filaments, their structural polarity was an advantage since each end could be independently targeted using functional groups or capping proteins. In the case of IFs, the apolar nature of the filament⁽²¹⁾ has always been a major difficulty, hence other approaches had to be devised to assay single-filament mechanics. In that respect, the most-promising technique is atomic force microscopy (AFM), with which it is possible to image, in physiological buffer, single IFs adsorbed to different solid supports.^(34,39) To extract mechanical information, the most-common experimental approach has been force spectroscopy, where the AFM tip is used to lift one portion of the sample above the surface. In this case, the sample is stretched between the solid support and the tip.^(65,66) Force spectroscopy

works well with polymers, modular proteins and unfolded polypeptide chains.^(67–69) Unfortunately, IFs adsorbed to a solid support do not detach from it⁽⁷⁰⁾ and instead the AFM tip extracts subunits from the filament surface.⁽⁷⁰⁾ This approach does not provide a direct measure of the tensile properties of single IFs but it may give invaluable information about the cohesive forces between the coiled-coil dimers within the filament.

A less-conventional approach is to increase the force applied by the AFM cantilever on the surface during a scan. This can lead to a mechanical perturbation of the filaments that is directly visible on the recorded image.⁽⁷¹⁾ Recently, this method was improved by first imaging a single neurofilament with the tip at low applied force, around 0.1 nN (Fig. 4A), and then increasing the applied force along only one scan line in order to “cut through” the filament (Fig. 4B).⁽⁷²⁾ Remarkably, in most cases, single neurofilaments stretched up to 3.5 times

their original length, i.e. 250% extension, before they ruptured (Fig. 4C).⁽⁷²⁾ This unusual extensibility was accompanied by a drastic reduction in the apparent width of the filaments (Fig. 4D), which is consistent with the model of an α -helix to β -sheet transition occurring in highly stretched filaments.⁽⁵⁸⁾ Similar results were obtained with two other types of IFs, desmin filaments and keratin filaments.⁽⁷²⁾ These experiments also confirm the most controversial observation that arose from the hagfish slime thread work, namely that individual IFs are far more extensible than previously assumed.⁽⁵⁸⁾ The next step will now be to measure the force applied to the filaments by the AFM tip during its movement. With the new generation of AFMs that include a “close-loop” scanner in three dimensions, this force can actually be determined by measuring variations in the cantilever torque while the sample is manipulated.⁽⁷³⁾ Preliminary data indicate that a stress–strain curve for a single IF can be extracted from

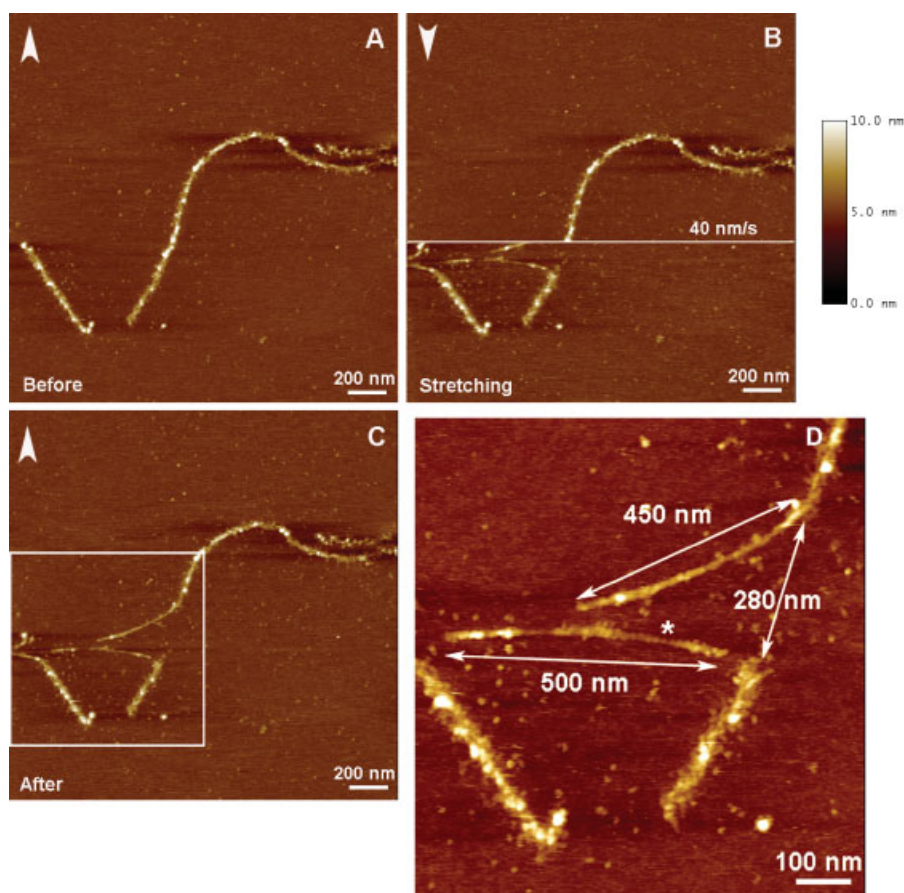


Figure 4. AFM manipulation of a single rat neurofilament adsorbed to mica. **A:** Control tapping mode AFM image of the filament before manipulation. The scanning orientation is indicated by the arrowhead. **B:** Along a single scan line, the applied force was increased in order to cut through the filament at a speed of 40 nm/s. **C,D:** As a result of the manipulation, a 280 nm long fragment was stretched into two pieces 455 and 500 nm in length, respectively. The resulting extension was 240%. The full width at half maximum of the stretched fragment was 12 nm compared to 30 nm for the unstretched filaments. A 8–10 nm banding pattern is visible along one of the stretched fragments (asterisk). Adapted from Kreplak L, Bär H, Leterrier JF, Herrmann H, Aebi U. 2005 *J Mol Biol* 354:569–577.

those measurements (L. Kreplak, unpublished observations). The only parameter that cannot be easily quantified by this experimental approach is the amount of energy that is dissipated by the surface-filament interaction during stretching.

To circumvent this difficulty, one might design an AFM experiment where a filament is deposited over 100 to 500 nm diameter hole. In this case, images taken at different applied forces may be recorded to extract a bending modulus from the measured deflection of the filament.⁽⁷⁴⁾ Using such an approach, the Young's and shear modulus for carbon nanotubes have been estimated by varying the diameter of the hole.⁽⁷⁴⁾ More recently, glutaraldehyde-fixed microtubules⁽⁷⁵⁾ were probed by the same experimental approach as well as fixed and unfixed vimentin IFs.⁽⁷⁶⁾ As a limitation, this approach can only provide a characterization of the mechanical properties in the elastic regime and therefore complements the large-strain stretching approach described above. Future improvements in mechanical testing at the nanoscale will no doubt lead to a better molecular understanding of IF mechanics at the single-filament level. This information, in turn, will have profound implications for a more rational understanding and possible treatment of human diseases that involve mutations in IF genes.^(77–80)

A molecular model of IF biomechanics

The next step is to propose a molecular description of the mechanical properties of several IF types over a wide range of strains. All the data presented above point to the fact that IFs

are flexible filaments⁽³⁴⁾ that are extensible individually⁽⁷²⁾ as well as within networks,⁽⁴³⁾ fibres⁽²⁵⁾ and bundles.⁽⁵⁸⁾ These mechanical properties can be accounted for by a simple molecular model.

To a first approximation, an IF is a bundle of laterally aligned α -helical coiled-coils. Depending on the interaction between the coiled-coils, two types of deformations can occur upon stretching. For small cohesive forces, the filament could shear, meaning that the coiled coils would slide past each other as the filament is lengthened. In this case, the stretching curve would possess a plateau at a force corresponding to the onset of slippage. Theoretically, the filament could be sheared to a single strand of coiled coils. Since, on average, one IF contains 16 coiled-coil dimers in cross-section, the maximal extension would be 1500%. Alternatively, if cohesive forces among coiled coils are high, shear would be negligible and the filament would behave as an elastic solid until the coiled coils start to unfold. In this case, the stretching curve would resemble the one for hair fibres, with a steep linear region to start with, a plateau corresponding to the unfolding of the coiled coils, and a final linear region before breakage. The maximal extension corresponding to complete unfolding of all the coiled-coils without any lateral slippage would be 150%.⁽⁷²⁾ The maximal extension observed for hagfish fibres and single filaments is 220% and 250%, respectively. According to the above reasoning, this could only be explained by some shearing of the filament structure. Interestingly, a limited shearing process has been proposed in the case of stretched hair fibres based on a small angle X-ray scattering study.⁽⁶³⁾ Other possible

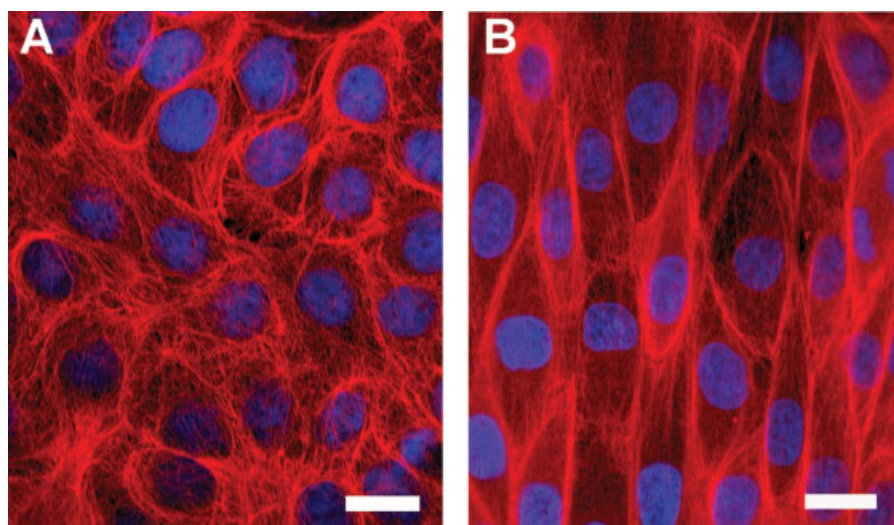


Figure 5. The effect of large-scale uniaxial stretch on the IF network in MDCK cells. Cells were grown on collagen-coated silastic membranes and stretched using a custom cell stretcher that was mounted on a confocal microscope. Cells were fixed and stained for immunofluorescence (red = keratin IFs, blue = DNA). **A:** Control cells were processed on a relaxed silastic membrane and **B:** stretched cells were fixed, stained and imaged on membranes that were held in the stretched state. Approximate uniaxial strain in stretched cells was 75%. Scale bar = 25 μ m.

Box 1. A short primer on biophysical terms and units.

In this paper, we discuss the material properties of IFs, which refers to how these filaments behave when they are subjected to mechanical forces. Physicists and materials scientists have defined a rich vocabulary of words (many of which were borrowed from the vernacular) so that the mechanical properties of materials can be directly and quantitatively compared to one another. Terms such as stress, strain, strength and toughness all have rigorous physical and mathematical definitions. Here we define the most important terms used in this review. A typical mechanical test involves pushing or pulling on an object and measuring the resultant force. By plotting force versus deformation, one can generate a graph that is quite informative about the mechanical behavior of that object. While the general shape of such a force–extension will be the same for different sized objects made from the same material, the magnitude of the forces and extensions will depend on size. For this reason, materials scientists came up with the concepts of strain and stress. **Strain** is simply a normalized value of extension. It is defined as the change in an object's length divided by its initial length, and is dimensionless. Similarly, force can be normalized by dividing by the cross-sectional area over which the force develops, and this is referred to as the **stress**. The typical units of stress are $\text{N} \cdot \text{m}^{-2}$, or Pa. The beauty of stress–strain curves is that they are similar for objects made of the same material, regardless of their size. They are also very useful for comparing the mechanical behavior of different materials. Many important aspects of a material's mechanical behavior can be derived from a stress–strain curve. The slope of a stress-strain curve indicates how much stress a material develops for a given amount of strain, and this is called the **stiffness**. For linearly elastic materials, the stiffness is often referred to as the **Young's Modulus**. The stress at which a material fails is called its **strength**, and the strain at which it fails is called its **extensibility**. The area under a stress–strain curve indicates the amount of strain energy that a material can absorb before it fails. This value is sometimes referred to as **toughness** and has units of $\text{J} \cdot \text{m}^{-3}$. The forces that materials develop when they are deformed arise generally from one of two mechanisms. **Enthalpic forces** arise from the straining of bonds, and result in an increase in the internal energy, or enthalpy of the material. In biological materials, enthalpic forces can arise from the straining of covalent bonds, hydrogen bonds, ionic interactions, and Van der Waals bonds. **Entropic forces** arise when the conformational entropy (a measure of the disorder of a system) of a material decreases. This phenomenon predominates in gels and rubber-like materials consisting of a network of cross-linked or entangled flexible molecules or filaments. We propose that the behavior of IF gels is dominated by entropic forces at low strains and enthalpic forces at higher strains when individual IFs experience direct longitudinal straining.

Box 2. Intermediate filaments as mechanically regulated signalling platforms?

The physiological roles of IFs have been mainly investigated using gene targeting in the mouse followed by a careful analysis of the resulting phenotype. One typical example is the desmin-null mouse, which is viable and fertile, but displays severe disruption of muscle architecture and myocardial degeneration. Specifically, desmin-null myofibrils show nuclei clustering⁽⁹⁵⁾ as well as disturbed mitochondrial positioning which leads to alterations in respiratory functions in situ.⁽⁹⁶⁾ Hence, these results confirm that desmin is involved in the structural and mechanical integration of muscle, and its absence may impact other functions that depend upon this structure. Simple epithelia such as the liver that are not subjected to large mechanical stresses offer a slightly different picture of IF function. K8/K18 IFs, which are expressed in simple epithelia, are important for embryonic development and the mechanical integrity of hepatocytes.^(87–89) However, studies of K8-null mice as well as mice expressing a K18 protein with a conserved arginine mutation demonstrate that this keratin pair performs additional roles. In these mice, the K8/K18 keratin pair seems to be involved in the resistance to Fas-mediated apoptosis and in the modulation of tumor necrosis factor (TNF) signalling.⁽⁹⁴⁾ Further evidence that K8/K18 filaments may behave as a signalling platform was provided by the discovery of their phosphorylation-dependent binding to 14-3-3 proteins.⁽⁹⁴⁾ However this signalling platform may be regulated by mechanical stresses. As discovered recently, shear stress, but not stretch, induces the disassembly of the K8/K18 filament network in alveolar epithelial cells via K8 phosphorylation by protein kinase C.⁽⁹⁷⁾ These findings suggest that the IF network may behave as a mechanically regulated signalling platform in simple epithelia. It is important to note that signalling and mechanical integration are not mutually exclusive functions, and the prominence of one over the other is most likely to be tissue dependent.

alternatives⁽⁵⁸⁾ involve deformation of the non- α -helical segments of the coiled-coil dimer⁽²¹⁾ or the N- or C-terminal end domains,⁽⁵⁸⁾ both of which would reduce the amount of shearing required to account for the large extensibility of IFs.

Despite the fact that our understanding of IF mechanics has made a quantum leap during the last few years, several questions remain. The most important goal at this point is to elucidate the stress–strain curve for single IFs. When this is achieved, the next step will be to understand the changes in molecular and supramolecular organization that occur when a single IF is stretched. Toward this end, one promising possibility is to assemble and stretch IFs containing a small proportion of fluorescently tagged proteins that could be used as reporters of molecular motions occurring under mechanical stress.

Biomechanical properties of IFs within cells and tissues

The extensive literature on wool biophysics provides detailed information about the biomechanics of fully keratinized cells, but there is still much to be learned about the contribution that IFs make to the mechanics of living cells and tissues. Using transgenic mouse models, investigators have demonstrated that IFs make a significant contribution to the stiffness of living cells^(81–84) and are important for the mechanical integrity of many tissues, including muscle, liver and skin.^(85–90) Interestingly, most of the studies published to date on cell mechanics have been based on experiments in which the applied strain was limited to only 20%.^(80,91–93) It is therefore not surprising that investigators have not detected the remarkable extensibility of IFs, which we now believe can be stretched to more than three times their resting length before breaking.^(58,72) Clearly a full understanding of the mechanical behaviour of IFs within cells requires deforming cells to higher maximum strains. To perform such experiments, we have designed and constructed a cell-stretching apparatus that allows us to apply uniaxial strains up to 140% on epithelial cells grown on silicone rubber membranes. Using immunofluorescence, it is then possible to characterize the deformation of the IF network spanning an epithelial cell (Fig. 5A,B). From preliminary experiments with this apparatus, we have found that the IF network appears remarkably robust, which is consistent with the mechanical data discussed above. We also have evidence that, at very large cell strains, deformation of the IF network is no longer elastic, but becomes plastic which, in turn, is consistent with the results of the hagfish slime thread data and recent AFM data (D. Fudge, D. Russell, E.B. Lane, A.W. Vogl, unpublished results). The next logical step will be to use stably transfected cell lines expressing fluorescently tagged IF proteins in order to characterize spatially and temporally the changes that occur in a mechanically deformed IF network. This model system will also be particularly relevant for elucidating the molecular mechanisms underlying the pathology of IF-related genetic diseases such as, for example, the skin-blistering disease Epidermolysis Bullosa Simplex (EBS).⁽⁸⁰⁾

Conclusion

Considering the unique mechanical properties observed for IFs both in vitro and in vivo within specific tissues, it is tempting to postulate an important role for them to translate mechanical stresses into a readable signal for the cell. For example, in bovine endothelial cells, a direct link between cytoplasmic IFs and the nuclear lamina has been demonstrated.⁽¹⁰⁾ If this linkage can be generalized to other cell types, it would offer a simple structural basis for mechanical signal transduction via the IF network. Another possibility is the mechanical activation of major cell signalling pathways. It is now fairly well accepted that IFs are involved in cell signalling as shown by several

transgenic mice studies.⁽⁹⁴⁾ What is now needed is convincing evidence of a direct link between a mechanical stress applied to the IF network and the activation or inactivation of major signalling pathway.

Acknowledgments

The authors would like to thank Ueli Aebi, John Gosline, Harald Herrmann and Wayne Vogl for unwavering support and fruitful discussions.

References

- Davies PF, Spaan JA, Krams R. 2005. Shear stress biology of the endothelium. *Ann Biomed Eng* 33:1714–1718.
- Discher DE, Janmey PA, Wang YL. 2005. Tissue cells feel and respond to the stiffness of their substrate. *Science* 310:1139–1143.
- Huang S, Ingber DE. 2005. Cell tension, matrix mechanics, and cancer development. *Cancer Cell* 8:175–176.
- Tarbell JM, Weinbaum S, Kamm RD. 2005. Cellular fluid mechanics and mechanotransduction. *Ann Biomed Eng* 33:1719–1723.
- Orr AW, Helmke BP, Blackman BR, Schwartz MA. 2006. Mechanisms of mechanotransduction. *Dev Cell* 10:11–20.
- Wang J, Zohar R, McCulloch CA. 2006. Multiple roles of alpha-smooth muscle actin in mechanotransduction. *Exp Cell Res* 312:205–214.
- Bloom S, Lockard VG, Bloom M. 1996. Intermediate filament-mediated stretch-induced changes in chromatin: a hypothesis for growth initiation in cardiac myocytes. *J Mol Cell Cardiol* 28:2123–2127.
- Helmke BP, Rosen AB, Davies PF. 2003. Mapping mechanical strain of an endogenous cytoskeletal network in living endothelial cells. *Biophys J* 84:2691–2699.
- Helmke BP, Thakker DB, Goldman RD, Davies PF. 2001. Spatiotemporal analysis of flow-induced intermediate filament displacement in living endothelial cells. *Biophys J* 80:184–194.
- Maniotis AJ, Chen CS, Ingber DE. 1997. Demonstration of mechanical connections between integrins, cytoskeletal filaments, and nucleoplasm that stabilize nuclear structure. *Proc Natl Acad Sci USA* 94:849–854.
- Lazarides E. 1980. Intermediate filaments as mechanical integrators of cellular space. *Nature* 283:249–256.
- Bär H, Strelkov SV, Sjöberg G, Aebi U, Herrmann H. 2004. The biology of desmin filaments: how do mutations affect their structure, assembly, and organisation? *J Struct Biol* 148:137–152.
- Dobb MG, Rogers GE. 1967. Electron microscopy of fibrous keratins. Symposium on fibrous proteins 1:267–278.
- Feughelman M. 1959. A two-phase structure for keratin fibres. *Textile Research Journal* 29:223–228.
- Fraser RD, MacRae TP, Rogers GE. 1972. Keratins: their composition, structure and biosynthesis, First ed. I.N. Kugelmas Springfield, IL: Charles C. Thomas.
- Gillespie JM, Frenkel MJ. 1974. The macroheterogeneity of type I tyrosine-rich proteins of Merino wool. *Aust J Biol Sci* 27:617–627.
- Astbury WT, Street A. 1931. X-ray studies of the structure of hair, wool and related fibres I. *General Trans Roy Soc* 230:75–101.
- Astbury WT, Woods HJ. 1933. X ray studies of the structure of hair, wool, and related fibres II. The molecular structure and elastic properties of hair keratin. *Phil Trans A* 232:333–394.
- Crick FHC. 1952. Is alpha-keratin a coiled coil? *Nature* 170:882–883.
- Pauling L, Corey RB. 1951. The structure of hair, muscle, and related proteins. *Proc Natl Acad Sci USA* 37:261–271.
- Strelkov SV, Herrmann H, Aebi U. 2003. Molecular architecture of intermediate filaments. *Bioessays* 25:243–251.
- Bendit EG. 1960. A quantitative X-Ray diffraction study of the alpha-beta transformation in wool keratin. *Textile Research Journal* 30:547–555.
- Kreplak L, Doucet J, Dumas P, Briki F. 2004. New aspects of the alpha-helix to beta-sheet transition in stretched hard alpha-keratin fibres. *Biophys J* 87:640–647.
- Akkermans RL, Warren PB. 2004. Multiscale modelling of human hair. *Philos Transact A Math Phys Eng Sci* 362:1783–1793.

25. Hearle JW. 2000. A critical review of the structural mechanics of wool and hair fibres. *Int J Biol Macromol* 27:123–138.
26. Morton WE, Hearle JW. 1993. *Physical Properties of Textile Fibres*. 3rd ed. Manchester: The Textile Institute.
27. Gittes F, Mickey B, Nettleton J, Howard J. 1993. Flexural rigidity of microtubules and actin filaments measured from thermal fluctuations in shape. *J Cell Biol* 120:923–934.
28. Kojima H, Ishijima A, Yanagida T. 1994. Direct measurement of stiffness of single actin filaments with and without tropomyosin by in vitro nanomanipulation. *Proc Natl Acad Sci USA* 91:12962–12966.
29. Felgner H, Frank R, Schliwa M. 1996. Flexural rigidity of microtubules measured with the use of optical tweezers. *J Cell Sci* 109:509–516.
30. Kurachi M, Hoshi M, Tashiro H. 1995. Buckling of a single microtubule by optical trapping forces: direct measurement of microtubule rigidity. *Cell Motil Cytoskeleton* 30:221–228.
31. Herrmann H, Kreplak L, Aebi U. 2004. Isolation, characterization, and in vitro assembly of intermediate filaments. *Methods Cell Biol* 78:3–24.
32. Herrmann H, Aebi U. 2004. Intermediate filaments: molecular structure, assembly mechanism, and integration into functionally distinct intracellular Scaffolds. *Annu Rev Biochem* 73:749–789.
33. Kreplak L, Aebi U, Herrmann H. 2004. Molecular mechanisms underlying the assembly of intermediate filaments. *Exp Cell Res* 301: 77–83.
34. Mücke N, Kreplak L, Kirmse R, Wedig T, Herrmann H, et al. 2004. Assessing the flexibility of intermediate filaments by atomic force microscopy. *J Mol Biol* 335:1241–1250.
35. Steinert PM, Zimmerman SB, Starger JM, Goldman RD. 1978. Ten-nanometer filaments of hamster BHK-21 cells and epidermal keratin filaments have similar structures. *Proc Natl Acad Sci USA* 75:6098–6101.
36. Herrmann H, Aebi U. 1998. Intermediate filament assembly: fibrillogenesis is driven by decisive dimer-dimer interactions. *Curr Opin Struct Biol* 8:177–185.
37. Hohenadl M, Storz T, Kirpal H, Kroy K, Merkel R. 1999. Desmin filaments studied by quasi-elastic light scattering. *Biophys J* 77:2199–2209.
38. Howard J. 2001. *Mechanics of Motor Proteins and the Cytoskeleton*. Sunderland, Massachusetts: Sinauer Associates.
39. Mücke N, Kirmse R, Wedig T, Leterrier JF, Kreplak L. 2005. Investigation of the morphology of intermediate filaments adsorbed to different solid supports. *J Struct Biol* 150:268–276.
40. Herrmann H, Hofmann I, Franke WW. 1992. Identification of a non-peptide motif in the vimentin head domain involved in intermediate filament assembly. *J Mol Biol* 223:637–650.
41. Hofmann I, Herrmann H, Franke WW. 1991. Assembly and structure of calcium-induced thick vimentin filaments. *Eur J Cell Biol* 56:328–341.
42. Norlen L, Al-Amoudi A, Dubochet J. 2003. A cryotransmission electron microscopy study of skin barrier formation. *J Invest Dermatol* 120:555–560.
43. Janmey PA, Euteneuer U, Traub P, Schliwa M. 1991. Viscoelastic properties of vimentin compared with other filamentous biopolymer networks. *J Cell Biol* 113:155–160.
44. Storm C, Pastore JJ, MacKintosh FC, Lubensky TC, Janmey PA. 2005. Nonlinear elasticity in biological gels. *Nature* 435:191–194.
45. Gardel ML, Shin JH, MacKintosh FC, Mahadevan L, Matsudaira PA, et al. 2004. Scaling of F-actin network rheology to probe single filament elasticity and dynamics. *Phys Rev Lett* 93:188102.
46. Onck PR, Koeman T, van Dillen T, van der Giessen E. 2005. Alternative explanation of stiffening in cross-linked semiflexible networks. *Phys Rev Lett* 95:178102.
47. Ma L, Xu J, Coulombe PA, Wirtz D. 1999. Keratin filament suspensions show unique micromechanical properties. *J Biol Chem* 274:19145–19151.
48. Bousquet O, Ma L, Yamada S, Gu C, Idei T, et al. 2001. The nonhelical tail domain of keratin 14 promotes filament bundling and enhances the mechanical properties of keratin intermediate filaments in vitro. *J Cell Biol* 155:747–754.
49. Yamada S, Wirtz D, Coulombe PA. 2003. The mechanical properties of simple keratins 8 and 18: discriminating between interfacial and bulk elasticities. *J Struct Biol* 143:45–55.
50. Downing SW, Spitzer RH, Koch EA, Salo WL. 1984. The hagfish slime gland thread cell. I. A unique cellular system for the study of intermediate filaments and intermediate filament-microtubule interactions. *J Cell Biol* 98:653–669.
51. Koch EA, Spitzer RH, Pithawalla RB, Parry DA. 1994. An unusual intermediate filament subunit from the cytoskeletal biopolymer released extracellularly into seawater by the primitive hagfish (*Eptatretus stouti*). *J Cell Sci* 107:3133–3144.
52. Downing SW, Salo WL, Spitzer RH, Koch EA. 1981. The hagfish slime gland: a model system for studying the biology of mucus. *Science* 214: 1143–1145.
53. Downing SW, Spitzer RH, Salo WL, Downing SD, Sidel LJ, et al. 1981. Hagfish slime gland thread cells: organization, biochemical features, and length. *Science* 212:326–327.
54. Fernholm B. 1981. Thread cells from the slime glands of hagfish (Myxiniidae). *Acta Zoologica* 62:137–145.
55. Spitzer RH, Koch EA, Downing SW. 1988. Maturation of hagfish gland thread cells: composition and characterization of intermediate filament polypeptides. *Cell Motil Cytoskeleton* 11:31–45.
56. Koch EA, Spitzer RH, Pithawalla RB, Downing SW. 1991. Keratin-like components of gland thread cells modulate the properties of mucus from hagfish (*Eptatretus stouti*). *Cell Tissue Res* 264:79–86.
57. Fudge DS, Levy N, Chiu S, Gosline JM. 2005. Composition, morphology and mechanics of hagfish slime. *J Exp Biol* 208:4613–4625.
58. Fudge DS, Gardner KH, Forsyth VT, Riekel C, Gosline JM. 2003. The mechanical properties of hydrated intermediate filaments: insights from hagfish slime threads. *Biophys J* 85:2015–2027.
59. Baden HP, Goldsmith LA, Lee L. 1974. The importance of understanding the comparative properties of hair and other keratinized tissues in studying disorders of hair. In: Brown AC, editor. *The first human hair symposium*. New York: Medcom Press. pp 388–398.
60. Park AC, Baddiel CB. 1972. Rheology of the stratum corneum: a molecular interpretation of the stress-strain curve. *J Soc Cosmet Chem* 23:3–12.
61. Fudge DS, Gosline JM. 2004. Molecular design of the alpha-keratin composite: insights from a matrix-free model, hagfish slime threads. *Proc Biol Sci* 271:291–299.
62. Tsuda Y, Yasutake H, Ishijima A, Yanagida T. 1996. Torsional rigidity of single actin filaments and actin-actin bond breaking force under torsion measured directly by in vitro micromanipulation. *Proc Natl Acad Sci USA* 93:12937–12942.
63. Kreplak L, Franbourg A, Briki F, Leroy F, Dalle D, et al. 2002. A new deformation model of hard alpha-keratin fibres at the nanometer scale: implications for hard alpha-keratin intermediate filament mechanical properties. *Biophys J* 82:2265–2274.
64. Liu X, Pollack GH. 2002. Mechanics of F-actin characterized with microfabricated cantilevers. *Biophys J* 83:2705–2715.
65. Abu-Lail NI, Camesano TA. 2003. Polysaccharide properties probed with atomic force microscopy. *J Microsc* 212:217–238.
66. Zlatanova J, Lindsay SM, Leuba SH. 2000. Single molecule force spectroscopy in biology using the atomic force microscope. *Prog Biophys Mol Biol* 74:37–61.
67. Aranda-Espinoza H, Carl P, Leterrier JF, Janmey PA, Discher DE. 2002. Domain unfolding in neurofilament sidearms: effects of phosphorylation and ATP. *FEBS Lett* 531:397–401.
68. Hansma HG, Kasuya K, Orudjev E. 2004. Atomic force microscopy imaging and pulling of nucleic acids. *Curr Opin Struct Biol* 14:380–385.
69. Rief M, Gautel M, Gaub HE. 2000. Unfolding forces of titin and fibronectin domains directly measured by AFM. *Adv Exp Med Biol* 481: 129–136.
70. Kiss B, Karsai A, Kellermayer MS. 2006. Nanomechanical properties of desmin intermediate filaments. *J Struct Biol* 155(2):327–339.
71. Brown HG, Troncoso JC, Hoh JH. 1998. Neurofilament-L homopolymers are less mechanically stable than native neurofilaments. *J Microsc* 191: 229–237.
72. Kreplak L, Bår H, Leterrier JF, Herrmann H, Aebi U. 2005. Exploring the mechanical behavior of single intermediate filaments. *J Mol Biol* 354: 569–577.
73. Guthold M, Liu W, Stephens B, Lord ST, Hantgan RR, et al. 2004. Visualization and mechanical manipulations of individual fibrin fibres

- suggest that fibre cross section has fractal dimension 1.3. *Biophys J* 87: 4226–4236.
74. Salvetat JP, Briggs GA, Bonard JM, Bacsa RR, Kulik AJ, et al. 1999. Elastic and shear moduli of single-walled carbon nanotube ropes. *Phys Rev Lett* 82:944–947.
75. Kis A, Kasas S, Babic B, Kulik AJ, Benoit W, et al. 2002. Nanomechanics of microtubules. *Phys Rev Lett* 89:248101.
76. Guzman C, Jeney S, Kreplak L, Kasas S, Kulik AJ, et al. 2006. Exploring the Mechanical Properties of Single Vimentin Intermediate Filaments by Atomic Force Microscopy. *J Mol Biol* 360:623–630.
77. Bår H, Mücke N, Kostareva A, Sjöberg G, Aebi U, et al. 2005. Severe muscle disease-causing desmin mutations interfere with in vitro filament assembly at distinct stages. *Proc Natl Acad Sci USA* 102:15099–15104.
78. Herrmann H, Wedig T, Porter RM, Lane EB, Aebi U. 2002. Characterization of early assembly intermediates of recombinant human keratins. *J Struct Biol* 137:82–96.
79. Rowat AC, Foster LJ, Nielsen MM, Weiss M, Ipsen J. 2005. Characterization of the elastic properties of the nuclear envelope. *Journal of the Royal Society Interface* 2:63–69.
80. Russell D, Andrews PD, James J, Lane EB. 2004. Mechanical stress induces profound remodelling of keratin filaments and cell junctions in epidermolysis bullosa simplex keratinocytes. *J Cell Sci* 117:5233–5243.
81. Beil M, Micoulet A, von Wichert G, Paschke S, Walther P, et al. 2003. Sphingosylphosphorylcholine regulates keratin network architecture and visco-elastic properties of human cancer cells. *Nat Cell Biol* 5:803–811.
82. Brown MJ, Hallam JA, Colucci-Guyon E, Shaw S. 2001. Rigidity of circulating lymphocytes is primarily conferred by vimentin intermediate filaments. *J Immunol* 166:6640–6646.
83. Trickey WR, Vail TP, Guilak F. 2004. The role of the cytoskeleton in the viscoelastic properties of human articular chondrocytes. *J Orthop Res* 22:131–139.
84. Wang N, Stamenovic D. 2000. Contribution of intermediate filaments to cell stiffness, stiffening, and growth. *Am J Physiol Cell Physiol* 279: C188–C194.
85. Baribault H, Price J, Miyai K, Oshima RG. 1993. Mid-gestational lethality in mice lacking keratin 8. *Genes Dev* 7:1191–1202.
86. Fuchs E, Esteves RA, Coulombe PA. 1992. Transgenic mice expressing a mutant keratin 10 gene reveal the likely genetic basis for epidermolytic hyperkeratosis. *Proc Natl Acad Sci USA* 89:6906–6910.
87. Hesse M, Franz T, Tamai Y, Taketo MM, Magin TM. 2000. Targeted deletion of keratins 18 and 19 leads to trophoblast fragility and early embryonic lethality. *Embo J* 19:5060–5070.
88. Ku NO, Michie S, Oshima RG, Omary MB. 1995. Chronic hepatitis, hepatocyte fragility, and increased soluble phosphoglycokeratins in transgenic mice expressing a keratin 18 conserved arginine mutant. *J Cell Biol* 131:1303–1314.
89. Loranger A, Duclos S, Grenier A, Price J, Wilson-Heiner M, et al. 1997. Simple epithelium keratins are required for maintenance of hepatocyte integrity. *Am J Pathol* 151:1673–1683.
90. Vassar R, Coulombe PA, Degenstein L, Albers K, Fuchs E. 1991. Mutant keratin expression in transgenic mice causes marked abnormalities resembling a human genetic skin disease. *Cell* 64:365–380.
91. Kippenberger S, Loitsch S, Guschel M, Muller J, Knies Y, et al. 2005. Mechanical stretch stimulates protein kinase B/Akt phosphorylation in epidermal cells via angiotensin II type 1 receptor and epidermal growth factor receptor. *J Biol Chem* 280:3060–3067.
92. Shirinsky VP, Antonov AS, Birukov KG, Sobolevsky AV, Romanov YA, et al. 1989. Mechano-chemical control of human endothelium orientation and size. *J Cell Biol* 109:331–339.
93. Takei T, Rivas-Gotz C, Delling CA, Koo JT, Mills I, et al. 1997. Effect of strain on human keratinocytes in vitro. *J Cell Physiol* 173:64–72.
94. Paramio JM, Jorcano JL. 2002. Beyond structure: do intermediate filaments modulate cell signalling? *Bioessays* 24:836–844.
95. Shah SB, Davis J, Weisleder N, Kostavassili I, McCulloch AD, et al. 2004. Structural and functional roles of desmin in mouse skeletal muscle during passive deformation. *Biophys J* 86:2993–3008.
96. Weisleder N, Taffet GE, Capetanaki Y. 2004. Bcl-2 overexpression corrects mitochondrial defects and ameliorates inherited desmin null cardiomyopathy. *Proc Natl Acad Sci USA* 101:769–774.
97. Ridge KM, Linz L, Flitney FW, Kuczmarski ER, Chou YH, et al. 2005. Keratin 8 phosphorylation by protein kinase C delta regulates shear stress-mediated disassembly of keratin intermediate filaments in alveolar epithelial cells. *J Biol Chem* 280:30400–30405.